一般セッション(口頭講演) | 10 スピントロニクス・マグネティクス：10.3 スピンデバイス・磁気メモリ・ストレージ技術

2025年3月14日(金) 13:30 ~ 17:15 K302 (講義棟)

[14p-K302-1~14] 10.3 スピンデバイス・磁気メモリ・ストレージ技術

河野 竜平(東北大)、 山野井 一人(慶應義塾大)

英語発表

13:30 ~ 13:45

[14p-K302-1]

High performance spin Hall sensing device using BiSb topological insulator

○(D)MIN LIU[1], Ruixian Zhang[1], Quang Le[2], Brian York[2], Cherngye Hwang[2], Xiaoyong Liu[2], Michael Gribelyuk[2], Xiaoyu Xu[2], Son Le[2], Maki Maeda[3], Tuo Fan[3], Yu Tao[3], Hisashi Takano[3], Pham Nam Hai[1] (1.Institute of Science Tokyo, 2.W Digital Inc., G.O., 3.W Digital Inc., F.)

奨励賞エントリー 英語発表

13:45 ~ 14:00

[14p-K302-2]

Pulse width dependence on Spin-Orbit Torque switching in an antiferromagnet Mn_3Sn thin film

○Shogo Yamada[1], Hanshen Tsai[1], Kouta Kondou[3], Yutaro Tsushima[1], Tomoya Higo[1,2], Satoru Nakatsuji[1,2,4,5] (1.Univ. of Tokyo, 2.ISSP, Univ. of Tokyo, 3.SRN, Osaka Univ., 4.JHU Phys. and Astron., 5.TSQS, Univ. of Tokyo)

14:00 ~ 14:15

[14p-K302-3]

Anisotropic spin-orbit torque unleashed by Fermi surface symmetry reduction

○杉本 聡志[1]、荒木 康史[2]、家田 淳一[2]、葛西 伸哉[1] (1.物材機構、2.原子力機構)

奨励賞エントリー 英語発表

14:15 ~ 14:30

[14p-K302-4]

Micromagnetic simulation study on the stability of sub-nano second magnetization switching for the long-axis angle of 75° in SOT-MRAM

○(D)Joonsoo Kim[1], Hiroshi Naganuma[2], Thi Van Anh Nguyen[1], Tetsuo Endoh[1] (1.Tohoku Univ., 2.Nagoya Univ.)

14:30 ~ 14:45

[14p-K302-5]

動的マグノニック結晶によるスピン波ギャップソリトンの特性評価

○(M2)田中 俊輔[1]、岩田 時弥[1]、関口 康爾[2] (1.横浜国大理工、2.横国大院工研)

14:45 ~ 15:00

[14p-K302-6]

垂直方向の磁気双極子結合を利用したマグノニック論理ゲート

○(M2)松井 拓磨[1]、林 龍之介[1]、羽田 拓真[1]、関口 康爾[2] (1.横浜国大理工、2.横浜国大院工)

英語発表

15:15 ~ 15:30

[14p-K302-7]

First-principles study of disordered effects and composition dependence on transport properties in $Co_2FeGa_{0.5}Ge_{0.5}$-CuZn based CPP-GMR devices

○(D)Kodchakorn SIMALAOTAO[1,2], Ivan Kurniawan[2], Yoshio Miura[2,3], Yuya Sakuraba[1,2] (1.Univ. of Tsukuba, 2.NIMS, 3.KIT)

🏷 英語発表

15:30 ~ 15:45

[14p-K302-8]

First-Principles Prediction for the Role of Rashba Spin-Orbit Coupling in Voltage-Controlled Magnetocrystalline Anisotropy on Fe/MgO

○(DC)Yosephine Novita Apriati[1], Masato Tsuchida[1], Kenji Nawa[1], Kohji Nakamura[1] (1.Mie Univ.)

🏷 英語発表

15:45 ~ 16:00

[14p-K302-9]

Cryogenic temperature deposition of a high-quality CoFe top-free layer for voltage-controlled magnetoresistive random-access memory

○Tomohiro Ichinose[1], Tatsuya Yamamoto[1], Takayuki Nozaki[1], Kay Yakushiji[1], Shingo Tamaru[1], Shinji Yuasa[1] (1.AIST)

🏷 英語発表

16:00 ~ 16:15

[14p-K302-10]

Microscopic study of MTJ degradation toward High-density STT-MRAM: Impact of interface Oxygen Frenkel defects in MgO barrier

○Rina Takashima[1], Takeo Koike[1], Shogo Itai[1], Hideyuki Sugiyama[1], Young Min Lee[1], Masaru Toko[1], Soichiro Ono[1], Daisuke Watanabe[1], Soichi Oikawa[1], Katsuhiko Koi[1], Hiroyuki Kanaya[1], Kohji Nakamura[2], Masahiko Nakayama[1] (1.Kioxia Corporation, 2.Mie Univ.)

🏷 奨励賞エントリー 🏷 英語発表

16:15 ~ 16:30

[14p-K302-11]

Tunneling magnetoresistance and spin-orbit torque magnetization switching in ferrimagnetic Gd-Fe-Co based magnetic tunnel junction

○(D)Masahiko Yunokizaki[1], Yuki Hibino[2], Hiroshi Idzuchi[1,3], Hanshen Tsai[1], Mio Ishibashi[1], Shinji Miwa[3,4], Masamistu Hayashi[1,4], Satoru Nakatsuji[1,3,4,5] (1.Dep. Phys., Univ. Tokyo, 2.AIST, 3.ISSP, Univ. Tokyo, 4.TSQS, Univ. Tokyo, 5.JHU)

🏷 奨励賞エントリー 🏷 英語発表

16:30 ~ 16:45

[14p-K302-12]

Size-Dependent Dynamic Properties of Stochastic Magnetic Tunnel Junction with a Synthetic Antiferromagnetic Free Layer

○(M1)Takuma Kinoshita[1], Ju-Young Yoon[1], Nuno Cacoilo[1], Haruna Kaneko[1], Shun Kanai[1], Hideo Ohno[1], Shunsuke Fukami[1] (1.Tohoku Univ.)

🏷 奨励賞エントリー 🏷 英語発表

16:45 ~ 17:00

[14p-K302-13]

Determination of coupling states of a spin-torque oscillator in an HDD head using injection locking

○Yuji Nakagawa[1], Hirofumi Suto[2], Yuya Sakuraba[2], Tomoyuki Maeda[1] (1.Toshiba, 2.NIMS)

奨励賞エントリー 英語発表

17:00 ~ 17:15

[14p-K302-14]

High-sensitivity and hysteresis-free tunnel magnetoresistance sensor with magnetic vortex structure

○(M2)Seiya Takano[1], Takafumi Nakano[1], Mikihiko Oogane[1,2] (1.Graduate School of Engineering, Tohoku Univ., 2.CSIS, Tohoku Univ.)

High performance spin Hall sensing device using BiSb topological insulator

[1] Institute of Science Tokyo, [2]Western Digital Inc., Great Oaks, [3]Western Digital Inc., Fujisawa
Min Liu[1], Zhang Ruixian[1], Quang Le[2], Brian York[2], Cherngye Hwang[2], Xiaoyong Liu[2], Michael Gribelyuk[2], Xiaoyu Xu[2], Son Le[2], Maki Maeda[3], Tuo Fan[3], Yu Tao[3], Hisashi Takano[3], Pham Nam Hai[1]
Email: liu.m.ag@m.titech.ac.jp

Recently, the spin Hall effect in non-magnetic materials with strong spin-orbit coupling has garnered significant attention as a promising approach for both manipulating and reading magnetic states. Notably, the “direct” spin Hall (DSH) effect has been extensively studied for its role in manipulating magnetic states within spin-orbit torque (SOT) MRAM. Conversely, its reciprocal counterpart, the “inverse” spin Hall (ISH) effect, has been investigated as a potential method for reading magnetic states in magnetic read head sensors used in hard-disk drives (HDD).[1)] In this work, we study a magnetic sensing device structure that utilizes the direct spin Hall (DSH) effect to read the magnetic state in a ferromagnetic (FM)/topological insulator (TI) heterostructure. From a materials perspective, employing quantum materials such as topological insulators[2)] or topological semimetals[3)] with a giant spin Hall angle offers significant advantages for device performance, as conventional heavy metals typically exhibit spin Hall angles below 1. We have fabricated a multilayer sample comprising a 3.8 nm buffer layer, a 9.7 nm BiSb TI layer, a 1.1 nm interlayer, a 0.8 nm-thick CoFe FM layer, and a capping layer, as shown in Fig. 1(a). We fabricated the DSH sensing device with two 40×40 μm^2 pillars on a 50 μm BiSb track, as shown in Fig. 1(b). In this structure, an in-plane DC charge current I_{DC} was injected into the Hall track along the x direction. We measured the voltage V_{DSH} between the electrode on top of the pillar and the bottom BiSb layer while sweeping an in-plane magnetic field along the y direction. As shown in Figs. 1(c) and 1(d), we found that while the output of our DSH sensing device is consistent with that of the ISH sensor, the spin Hall angle calculated from its magnitude (θ_{SH} ~ 164) is colossal and significantly higher than that (θ_{SH} ~ 3.5) obtained from second harmonic measurement.[4)] Our findings show that the giant DSH and ISH effects in TI-based heterostructure are reciprocal and hold great potential for next-generation magnetic read head sensors and other SOT devices.

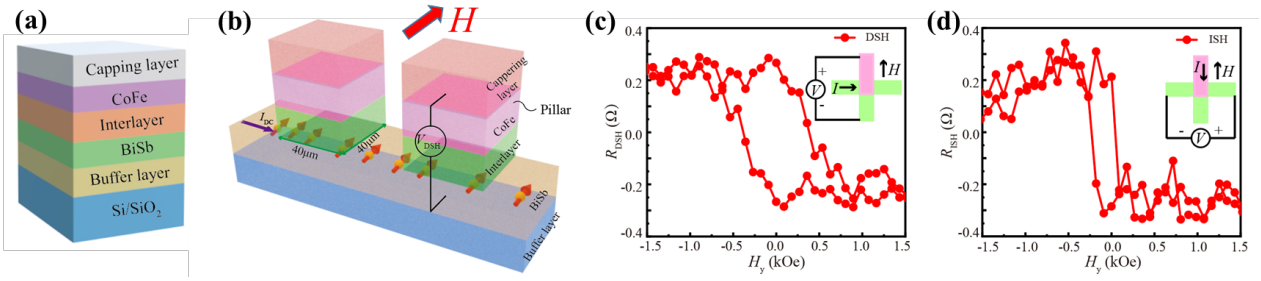

Figure 1. Schematic illustration of (a) the multilayer stack and (b) the direct spin Hall sensing device structure and the measurement setup. (c) R_{DSH} and (d) R_{ISH} measured at I_{DC} = 0.2 mA.

References
1) H. H. Huy, J. Sasaki, N. H. D. Khang, S. Namba, P. N. Hai, *et al.*, Appl. Phys. Lett. 122, 052401 (2023).
2) N. H. D. Khang, Y. Ueda, P. N. Hai, Nat. Mater. 9, 808 (2018).
3) T. Shirokura, T. Fan, N.H.D. Khang, T. Kondo, P. N. Hai, Sci. Rep. 12, 2426 (2022).
4) M. Liu, Z. Ruixian, Q. Le, B. York, C. Hwang, X. Liu, *et al.*, Appl. Phys. Lett. 125, 242401 (2024).

Pulse width dependence on Spin-Orbit Torque switching in an antiferromagnet Mn_3Sn thin film

○Shogo Yamada[1], Hanshen Tsai[1], Kouta Kondou[2], Yutaro Tsushima[1], Tomoya Higo[1,3] & Satoru Nakatsuji[1,3,4,5]

Univ. of Tokyo[1], SRN, Osaka Univ.[2], ISSP, Univ. of Tokyo[3], JHU Phys. and Astron.[4], TSQS, Univ. of Tokyo[5]

E-mail: yamadasy35@g.ecc.u-tokyo.ac.jp

The electrical manipulation of the magnetic order is essential for the application of spintronic devices, particularly non-volatile magnetic random access memory (MRAM). Compared to conventional devices based on ferromagnets, antiferromagnets have higher response speeds and lower stray fields, so they are promising materials for the next-generation MRAM. In particular, topological antiferromagnet Mn_3Sn has Weyl nodes near the Fermi level and its characteristic octupole breaks time-reversal symmetry, so it shows a large anomalous Hall effect (Fig. A) [1]. Recently, electrical manipulation has been realized by the Spin-Orbit Torque (SOT) switching in Mn_3Sn and heavy metal heterostructures at room temperature (Fig. B) [2,3].

However, since the Mn_3Sn layer (>10nm, usually) is far thicker than the magnetic layer of conventional ferromagnetic devices (~ a few nm), we cannot neglect the Joule heating generated by the electrical pulse. For example, in the 40nm Mn_3Sn layer, it reaches almost its Neel temperature of ~ 420K [4]. It also shows less switching in shorter pulses. These results suggest that Mn_3Sn loses its magnetic order and cannot work particularly in high-speed, sub-ns regions, which prevents its application.

Here, the film is Mn_3Sn (15nm) /Ta (5nm) /Al_2O_3 (3nm) from the substrate side. We find that the threshold current density and the switching rate is different between 10ns pulse and 100ns pulse (Fig. C). It shows larger switching in a shorter pulse. This result suggests that there is an important change in the switching mechanism among different pulse widths.

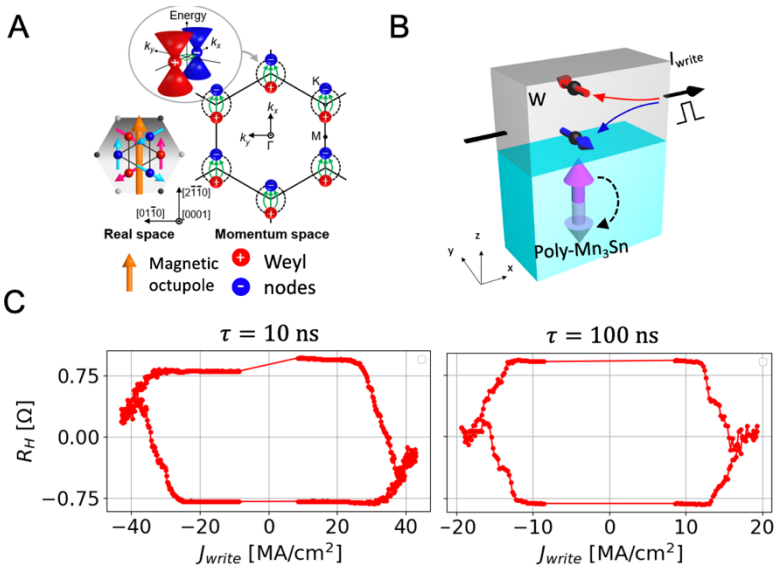

(A)Magnetic octupole and Weyl nodes distribution in Mn_3Sn
(B)SOT switching in the heavy metal/Mn_3Sn heterostructure
(C)Pulse width dependence on threshold current density. Pulse amplitude vs Hall resistance hysteresis (insets).

[1] Nakatsuji, S., Kiyohara, N. & Higo, T. *Nature* **527**, 212–215 (2015).
[2] Tsai, H., Higo, T., Kondou, K. *et al. Nature* **580**, 608–613 (2020).
[3] Higo, T., Kondou, K., Nomoto, T. *et al. Nature* **607**, 474–479 (2022).
[4] B. Pal *et al*. *Sci*. *Adv*. **8**, eabo5930 (2022).

Anisotropic spin-orbit torque unleashed by Fermi surface symmetry reduction

◦(P)S. Sugimoto[1], Y. Araki[2], J. Ieda[2], and S. Kasai[1,3]

(1. NIMS, 2. JAEA, 3. JST PRESTO)

E-mail: SUGIMOTO.Satoshi@nims.go.jp

The design of spin polarization is an essential agenda for further development of spin-orbit torque (SOT) applications. In typical heterostructure systems, the spin polarizations in SOT usually lack the out-of-plane (OOP) and one of the in-plane (IP) components, leading to nondeterministic switching problems at type-*z* and type-*x* configurations [1,2]. Unleashing these unconventional SOTs generally requires further symmetry reduction in thin-film layered structures. Here, we introduce a new approach to induce huge OOP and IP SOTs in Bi_2Te_3/CoFeB heterostructures, by employing a simple but powerful symmetry reduction protocol for the Fermi surface structure of the interfacial electrons.

Epitaxial Bi_2Te_3 (001) films were fabricated using a magnetron sputtering system on sapphire substrates. The systems belong to the *R*-3*m* space group, leading to the threefold symmetry (C_{3V}) in the interfacial Fermi surface instead of the continuous rotational symmetry ($C_{\infty V}$) [Fig. 1(a)]. We further elaborated an atomic-scale thickness gradient $\Delta t = (3\pm1)$ Å, which effectively acts as an in-plane orthogonal perturbation reducing the symmetry down to the trivial C_1 group [Fig. 1(b)]. Such a symmetry reduction fully removes the geometric constraints of laminated devices, unleashing finite OOP and IP SOTs [3]. Figures 1(c) and (d) show FMR spectra observed in W/CoFeB belonging to $C_{\infty V}$, and wedge-shaped Bi_2Te_3/CoFeB to C_1, respectively. A clear nonreciprocity upon the magnetic field inversion was seen uniquely to the C_1 structure, indicating the onset of unconventional SOTs. The in-plane torque profiles revealed the emergence of strong field-like and damping-like SOTs including both OOP and IP components. Moreover, their spin-to-charge conversion efficiencies ζ_i ($i = x,y,z$) were quantified to be comparable to those in heavy metals ($\zeta_{x(z)} \sim 0.1$). Such strong $\zeta_{x(z)}$ are beneficial for the deterministic SOT switching at zero magnetic field.

[1] I. M. Miron *et al.*, Nature (London) **476**, 189 (2011). [2] S. Fukami *et al.*, Nat. Nanotechnol. **11**, 621 (2016). [3] S. Sugimoto, Y. Araki *et al.*, accepted for publication in Commun. Phys.

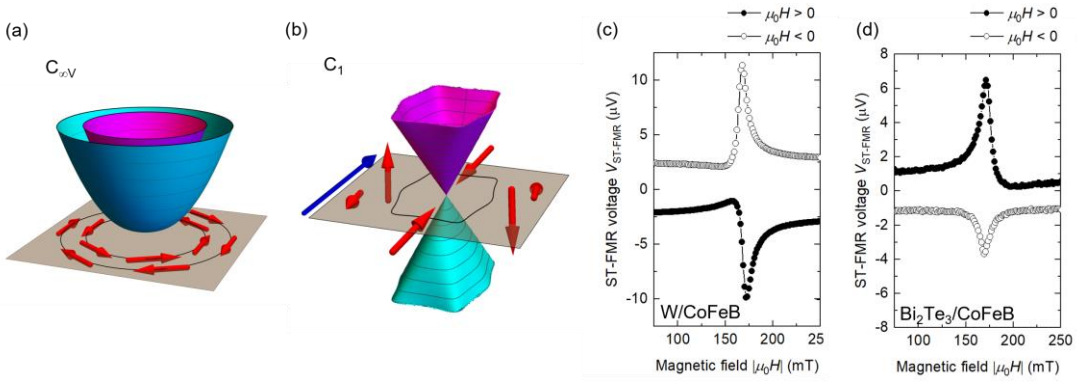

Fig. 1 Schematized Fermi surfaces for (a) $C_{\infty V}$ and (b) C_1 symmetries. FMR spectra for (c) W/CoFeB heterostructures to $C_{\infty V}$ and (d) wedge-shaped Bi_2Te_3/CoFeB heterostructures to C_1.

Micromagnetic simulation study on the stability of sub-nano second magnetization switching for the long-axis angle of 75° in SOT-MRAM

Tohoku Univ. [1], Nagoya Univ., [2] ○Joonsoo Kim[1], H. Naganuma[2], T. V. A. Nguyen[1], T. Endoh[1]

E-mail: kim.joonsoo.p2@dc.tohoku.ac.jp

Spin-Orbit Torque Magnetic Random Access Memory (SOT-MRAM) is a promising candidate for next-generation non-volatile memory due to its fast-switching speed, low power consumption, and scalability. This presentation focuses on the effects of the long-axis tilt angle of magnetic tunnel junction (MTJ) with ellipse shape on the magnetization switching behavior in the SOT-MRAM devices, analyzed through micromagnetic simulations. The micromagnetic simulations[1)] were conducted to evaluate the stability and efficiency of sub-nanosecond magnetization switching under varying voltage levels and long-axis tilt angles. [Fig. 1] The results reveal that at smaller tilt angles, such as 15°, the generation of spin torque decreases during the initiation of magnetization switching but increases significantly near the end of the process. This uneven behavior leads to back-hopping and destabilizes the magnetization switching. In contrast, a tilt angle of 75° achieves optimal performance, enabling fast and stable magnetization switching. The stability switching is due to reducing spin torque just after switching. The quantitative analysis of spin torque coefficients highlights the critical role of angle-dependent spin torque generation in achieving reliable switching at 75°. This work provides a detailed understanding of angle-dependent magnetization switching in SOT-MRAM devices and underscores the importance of structural design for enhancing device performance.

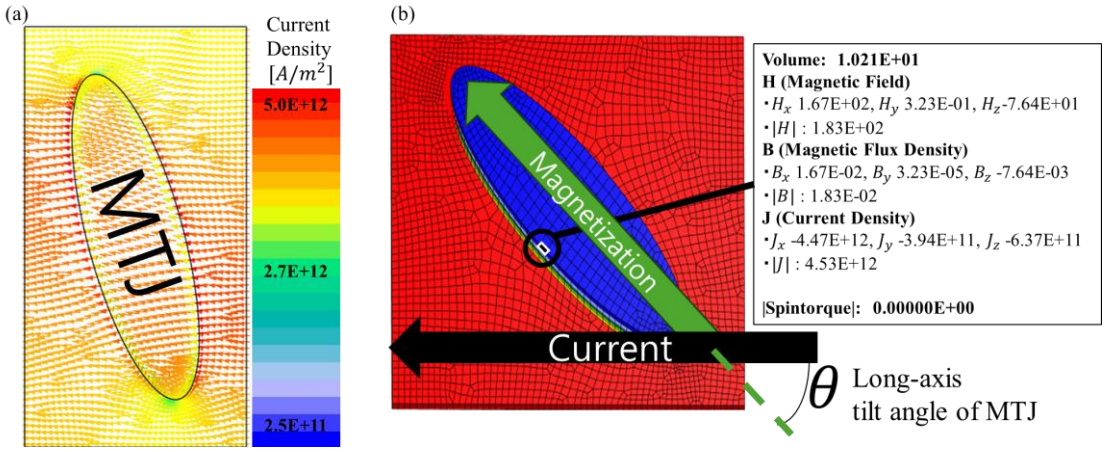

Figure 1. (a) Micromagnetic simulation showing the current flow and charge density in an SOT device. (b) The mesh structure visualizes the electromagnetic properties at different positions. The angle θ represents the tilt angle of the magnetic tunnel junction (MTJ), affecting spin torque and magnetization switching.

This work was supported in part by the CIES Industrial Affiliation on STT MRAM Program, the CIES Consortium, and NEDO-AI, X-nics, and JSPS core to core program (No. JPJSCCA20230005).

Reference 1) T.V.A. Nguyen, H. Naganuma, H. Honjo, T. Endoh, *AIP Advances* **14**, 025018 (2024).

動的マグノニック結晶によるスピン波ギャップソリトンの特性評価

Characterization of spin wave gap solitons in dynamic magnonic crystals

横国大理工，○(M2)田中 俊輔，(M1)岩田　時弥，関口　康爾
Yokohama National Univ., ○Shunsuke Tanaka, Tokiya Iwata, and Koji Sekiguchi
E-mail: tanaka-shunsuke-wd@ynu.jp

角運動量の流れ（スピン波）を扱うマグノニクス分野では、波として位相と振幅の情報を同時に伝搬させることでジュール熱が発生しない情報処理が期待されている。スピン波ソリトンには、周波数に対する分散効果の曲率と、波の振幅による周波数変化との関係から引力的な非線形性をもち波形が急峻化するブライトソリトンと、斥力的な非線形性をもち波形の存在しない領域が急峻化するダークソリトンの二種類があり、試料に対する外部磁場の印加方向によってどちらかのソリトンが選択される。しかしながら、導波路に周期的な溝をエッチングした静的マグノニック結晶と呼ばれるスピン波制御法を用いることで、特定の周波数帯における減衰バンドを生成し、バンド内で形成されるスピン波ソリトンの種類が逆転することが報告された[1]。そこで本研究ではスピン波導波路に周期的な変調磁場を発生させ信号を減衰させる動的マグノニック結晶を用いて、形成したスピン波ソリトンの特性を評価した[2]。

実験基板を Fig. 1 に示す。導波路として厚さ 5.1 μm、幅 2 mm、長さ 13 mm のイットリウム鉄ガーネット (YIG) を使用した。アンテナ間距離は 8 mm である。スピン波の進行方向に対し面内垂直方向に外部磁場 H_{ex}（= 122 mT）を印加し、コンバイナを用いて幅 450 μm の入力アンテナに周波数の異なる 2 つの連続波信号（f_1 = 5254.3 MHz、f_2 = 5285.3 MHz）を印加することで誘導変調不安定性によりスピン波ソリトンを形成した。アンテナ間に周期構造を配置して I = 0.6 A の電流を印加することで変調磁場を導波路表面に印加した。周期構造を通過したスピン波の誘導起電力を検出し、リアルタイムオシロスコープを用いて実時間波形の測定を行った。

リアルタイムオシロスコープによる実時間波形を Fig. 2 (a)、2(b) に示す。f_1 と f_2 の連続波誘導変調において、ダークソリトンに有意な波形の溝が急峻となる Fig. 2 (a) が観測され、周期構造に I = 0.6 A の直流電圧を印加することで Fig. 2 (b) のようなブライトソリトンの波形変化があった。斥力的な非線形をもちダークソリトンが支配的となる Surface mode でのスピン波ソリトン励起に対しブライトソリトンが出現した原因として、伝送損失により f_1 、f_2 における分散効果 D の符号（曲率）が逆転したことで、検出波形が引力的な非線形性をもつブライトソリトンに変化したことが考えられる。

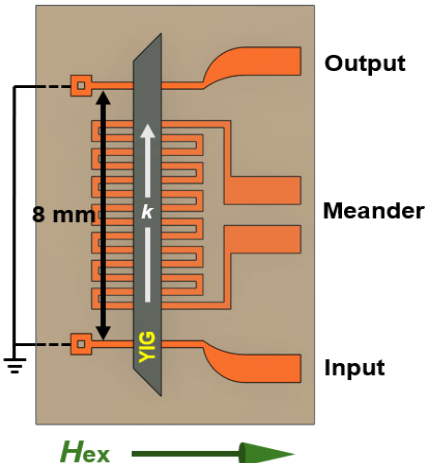

Fig. 1 : Schematic of the experiment device.

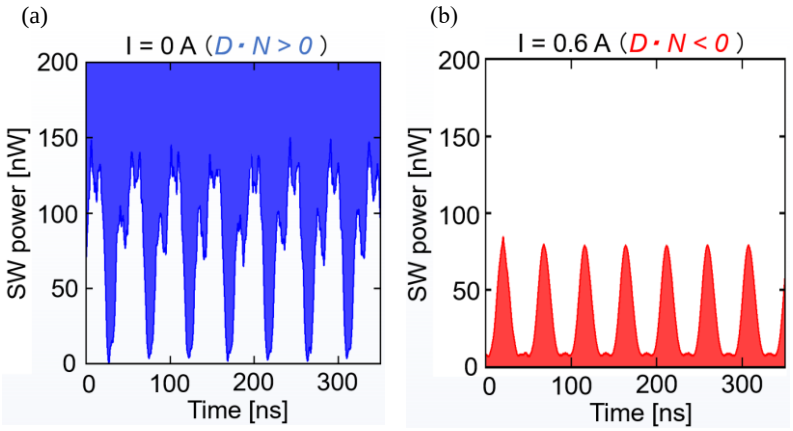

Fig. 2 : (a) (b) Time-domain waveforms of spin wave soliton.

References

1) M. Wu, B. A. Kalinicos, and C. E. Patton, *Phys Rev Lett.*, **93**, 157207 (2004).
2) M. Iwaba, K. Sekiguchi, 2021 *Appl. Phys. Express.* **14**, 073002 (2021)

垂直方向の磁気双極子結合を利用したマグノニック論理ゲート

Magnonic logic gate using a perpendicular magnetic dipole coupling

横浜国立大学 大学院理工学府[1], 横浜国立大学 大学院工学研究院[2]
○(M2)松井 拓磨[1], 林 龍之介[1], (M2)羽田 拓真[1], 関口 康爾[2]
Graduate school of engineering Yokohama national university[1], Faculty of engineering Yokohama national university[2], ○Takuma Matsui[1], Ryuunosuke Hayashi[1], Takuma Hada[1], and Koji Sekiguchi[2]
E-mail: matsui-takuma-dg@ynu.jp

スピン波は磁化の歳差運動によりスピン角運動量が伝搬する現象である。電荷の移動を伴わないスピン波は超低消費電力な新たな情報キャリアとして注目されており、情報処理デバイスに関する様々な研究が進められている[1, 2]。しかし、スピン波は伝搬に伴う振幅減衰が顕著であることから、長距離伝搬は困難であり、長さ方向への拡張には限界がある。本研究では、磁気双極子結合に着目し[3]、垂直方向への拡張が可能となる新たなデバイス構造を提案する。膜厚方向にギャップを持つ磁気双極子結合を利用した 2 層構造のスピン波演算デバイスを作製し、時間分解電気測定により、スピン波伝搬特性を調査した。

Fig. 1 に作製したスピン波デバイスと実験模式図を示す。酸化膜付き Si 基板上に、1 層目として Py 薄膜(膜厚 35 nm)を RF マグネトロンスパッタリングによって成膜し、Ar イオンミリングによって幅 120 μm、長さ 200 μm の矩形を 10 μm 間隔で 2 つ作製した。SiO_2(35 nm)によって矩形の間隔を埋め戻し、導波路上に絶縁層としてSiO_2(20 nm)を成膜した後、2 層目のスピン波導波路として Py(35 nm)を成膜した。シグナル線幅 3 μm のマイクロ波アンテナを真空蒸着法により Ti(5 nm)/Au(100 nm)で作製し、導波路の幅方向に外部磁場H_{ex}を印加し、励起アンテナ 1 に 7.5V の矩形波パルスを入力することで、1 層目のスピン波演算デバイスに表面スピン波(MSSW)を励起し、2 層目の導波路に伝搬したスピン波をサンプリングオシロスコープによって電気的に検出した。

Fig. 2 は、外部磁場H_{ex}を 50~300 Oe まで 50 Oe 刻みで印加したときの検出アンテナで取得した実時間波形である。黒矢印で示した信号パケットによって、外部磁場の増加に伴う到達時間の変化が観測できた。実時間波形に対してフーリエ解析を行った結果を Fig. 3 に示す。実験によって得られた各外部磁場に対する共鳴周波数との関係を MSSW の分散関係の理論値と比較した結果、波数$k = 0.39\ \mathrm{rad/\mu m}$が算出され、実験値と理論値の一致が確認できた。これらの結果から、MSSW が垂直方向のギャップを越えて伝搬したことがわかった。

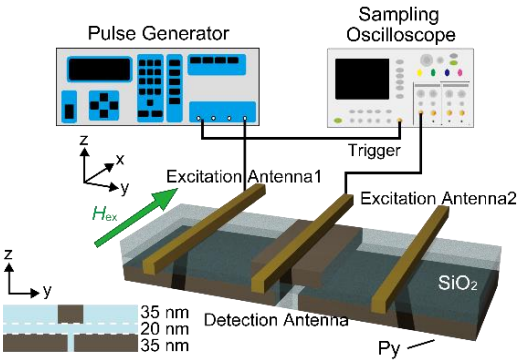

Fig. 1 : A schematic diagram of experimental setup

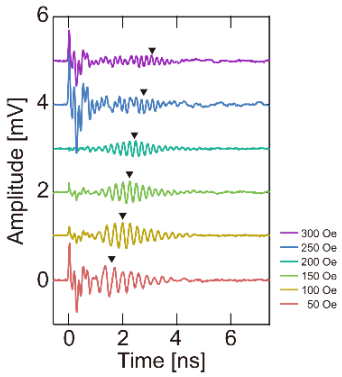

Fig. 2 : Output profiles of detected spin wave real-time waveforms for different external magnetic fields.

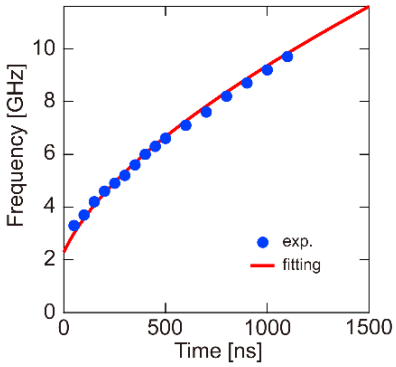

Fig. 3 : Spin wave resonance frequency as a function of a magnetic field. The closed circles are experimental values. The solid line is a calculation fitting result.

References

[1] N. Kanazawa, T. Goto, K. Sekiguchi *et al.*, *Sci. Rep.* **7**, 7898 (2017)
[2] T. Goto, T. Yoshimoto, B. Iwamoto, *et al.*, *Sci. Rep.* **9**, 16472 (2019)
[3] R. Hayashi, S. Nezu and K. Sekiguchi, *Phys. Rev. Appl.* **22**, 034037 (2024)

First-principles study of disordered effects and composition dependence on transport properties in $Co_2FeGa_{0.5}Ge_{0.5}$-CuZn based CPP-GMR devices

University of Tsukuba[1], NIMS[2], Kyoto Institute of Technology[3]

°Kodchakorn Simalaotao[1,2], Ivan Kurniawan[2], Yoshio Miura[2,3], Yuya Sakuraba[1,2]

E-mail: s2330100@u.tsukuba.ac.jp

Current-perpendicular-to-plane giant magnetoresistance (CPP-GMR) devices are emerging as promising candidates for next-generation magnetic read heads in hard disk drives (HDDs) due to their low resistance-area product (RA) and compatibility with high-speed operations[1-2]. Building on our previous work, we conducted a systematic search of Cu-X binary spacers and identified CuZn as the optimal candidate for integration with half-metallic $Co_2FeGa_{0.5}Ge_{0.5}$ (CFGG) electrodes. This was attributed to their significant conductive states, particularly around the $k_{||}$ = (0,0) in the Brillouin zone, and their good Fermi surface matching with CFGG electrodes. In this study, we extend the investigation to explore the effects of atomic disorder and composition dependence in CuZn spacers on the majority-spin ballistic conductance, inversely proportional to interfacial resistance. Across the degree of disorder x ($0 \le x \le 1$) (with Cu site: $Cu_{1-x}Zn_x$ and with Zn site: Cu_xZn_{1-x}), where the CuZn spacer transitions from B2 (Zn-terminated) to A2 and finally to B2 (Cu-terminated) structures, the conductance was observed to strongly depend on both the degree of disorder and the termination type at the CFGG/CuZn interface (Fig. 1 (a)). For FeGe- and FeGa-terminated configurations, the conductance increases linearly with disorder degree x, while Co-terminated structures show a weaker dependence. Among all configurations, the B2-ordered Cu-terminated spacer with FeGa termination shows the highest conductance enhancement, approximately 3%, compared to the A2-disordered spacer. In addition, the compositional dependence of $Cu_{1-y}Zn_y$ ($0 \le y \le 1$) spacers was analyzed for B2- and A2-type structures (Figure 1 (b)-(d)). The results indicate that majority-spin ballistic conductance is maximized at approximately 35–50% Zn content for both structure types. These findings highlight the critical role of atomic disorder and composition in determining transport properties, offering key insights for the atomic-scale design of spacer materials and interfaces in high-performance CPP-GMR devices.

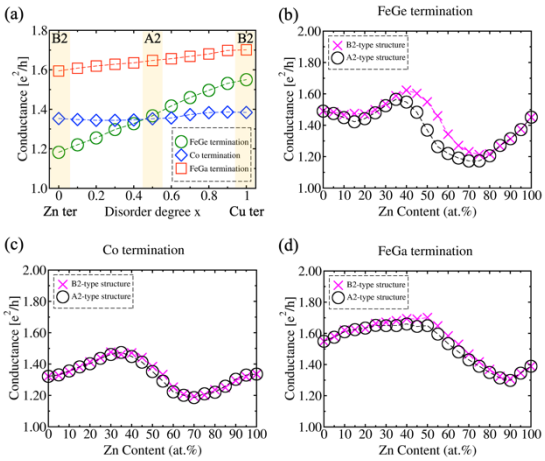

Fig. 1 (a) Average majority-spin conductance as a function of degree of disorder x ($0 \le x \le 1$) for FeGe, Co, and FeGa electrode terminations. Average majority-spin conductance as a function of Zn content for (b) FeGe, (c) Co, and (d) FeGa electrode termination, shown for both B2 and A2-type structures.

References

1. Z. Diao, *et al.*, J. Magn. Magn. Mater. **356,** 73 (2014).
2. Büker, B., *et al.,* Phys. Rev. B, **103**, L140405 (2021).

First-Principles Prediction for the Role of Rashba Spin-Orbit Coupling in Voltage-Controlled Magnetocrystalline Anisotropy on Fe/MgO

Mie Univ. , ○Yosephine Novita Apriati, Masato Tsuchida, Kenji Nawa, Kohji Nakamura

E-mail: yosephinetha.work.rc@gmail.com

The demand for higher density, higher speed, and lower energy magnetoresistive random access memory faces two grand challenges: first, acquire a voltage-controlled magnetocrystalline anisotropy (VCMA) efficiency >1000 fJ/Vm; second, achieve perpendicular magnetocrystalline anisotropy (PMA) >2 mJ/m^2 [1,2]. The–mechanism of VCMA is mainly attributed to the modifications of the occupied states and electric-field-induced changes in magnetic dipole moments. In metal/insulator systems, however, the inversion symmetry breaking due to the contrast electrostatic potential at the interface leads to Rashba spin-orbit coupling (SOC) which is odd in momentum ***k***-space and can not be ignored. Here, we revisit and clarify the role of Rashba SOC in Fe/MgO-based magnetic tunnel junctions (MTJs) specifically for VCMA and PMA. Efforts to achieve large VCMA-coefficients have been ongoing, including the incorporation of hybrid MgO-based tunnel barriers with various insulating materials, e.g., alkali halides [2], high-dielectric constant materials [3], and piezoelectric materials [4]. The pristine system of Fe/MgO is modeled by ten atomic monolayers (ML) of Fe(001) and five ML MgO(001). All calculations are performed using the full-potential linearized augmented plane-wave (FLAPW) method [5], with the systems analyzed under an external bias voltage (V_{ext}) ranging from -0.4 to +0.4 V/Å in vacuum regions. The PMA energy of 0.32 mJ/m^2 with a VCMA-coefficient of 32.1ε fJ/Vm, where the ε is dielectric constant of the tunnel barrier, is observed. The PMA originates from the occupied *d* band around Fermi energy (E_F). The *d* band is odd when the SOC is accounted for in-plane magnetization direction change from *+x* to *-x*, indicating the Rashba band effect. When the V_{ext} is applied, the Rashba band shifts according to the magnitude of the V_{ext}, leading to the change in PMA energy that is attributed to the origin of the VCMA-coefficient. The work further explores the potential of tailoring the VCMA-coefficient via the Rashba effect by controlling electric polarity at the Fe/MgO interface, e.g., by incorporating a LiF or an AlN ML on the interface, which shows that it is possible to control the VCMA-coefficient directly by modifying the energy shift of the Rashba band.

[1] Wang. K.L, *et. al*., J. Phys. D: Appl. Phys., **46** (2013), 074003.

[2] Shao. Y. and Amiri. K., Adv. Mater. Technol., **8** (2023), 2300676.

[2] Chen. J, *et.al*., Phys. Rev. B., **107** (2023), 094420.

[3] Onoda. H., *et. al*., Appl. Phys. Express., **17** (2024), 023001.

[4] Chien. D., *et. al*., Appl. Phys. Lett., **108** (2016), 112402.

[5] Nakamura. K., *et.al*., Phys. Rev. B., **67** (2003), 014420.

Cryogenic temperature deposition of a high-quality CoFe top-free layer for voltage-controlled magnetoresistive random-access memory

AIST [1], ◦Tomohiro Ichinose[1], Tatsuya Yamamoto[1], Takayuki Nozaki[1], Kay Yakushiji[1], Shingo Tamaru[1], Shinji Yuasa[1]

E-mail: tomohiro.ichinose@aist.go.jp

To implement a magnetoresistive random-access memory in practical devices, it is of great importance to develop high-quality top-free type magnetic tunnel junctions (MTJs). As the top-free layer, amorphous CoFeB has been used even though crystalline materials possess rich potential such as large bulk perpendicular magnetic anisotropy (PMA), half-metallic band structures, and high voltage-controlled magnetic anisotropy (VCMA) efficiency. [1] The main reason for this comes from the difficulty in fabricating a high-quality crystalline ultrathin film on a MgO tunneling barrier. In this work, the high-quality crystalline CoFe top-free layer was developed using cryogenic temperature deposition and a Fe-substituted MgO (MgFeO) barrier.

Typical MTJs in this study were comprised of [hard Co/Pt]/Ir(0.48)/Co(0.85)/Mo(0.3)/CoFeB(0.8)/[MgO(1.7) or MgO(0.4)/$Mg_{40}Fe_{10}O_{50}$(1.3)]/$Co_{50}Fe_{50}$(t_{CoFe})/MgO(1) multilayers (thicknesses in nm), which were deposited on ϕ300 mm Si/SiO_2 wafers using a mass-production-compatible sputtering system (EXIM, Tokyo Electron Ltd.). The CoFe free layer was deposited at T_{CoFe} = 300 or 100 K. The structural and magnetic properties of the MTJs were investigated using scanning transmission electron microscopy (STEM), vibrating sample magnetometry, and ferromagnetic resonance measurements. A probe station was used to investigate the magnetotransport properties of the MTJ devices.

STEM analyses revealed that the CoFe layer deposited at 300 K exhibited a rough and ambiguous interface due to the island-like growth of CoFe on a MgO layer. The island-like growth of CoFe was effectively suppressed using cryogenic temperature deposition at 100 K. The suppression of island-like growth resulted in improved magnetic properties as shown in figure 1. Further improved device performances such as PMA, magnetic damping, and tunnel magnetoresistance were obtained by using a MgFeO barrier instead of MgO. We also present the effect of Ir-doping on the VCMA effect and voltage-driven magnetization switching.

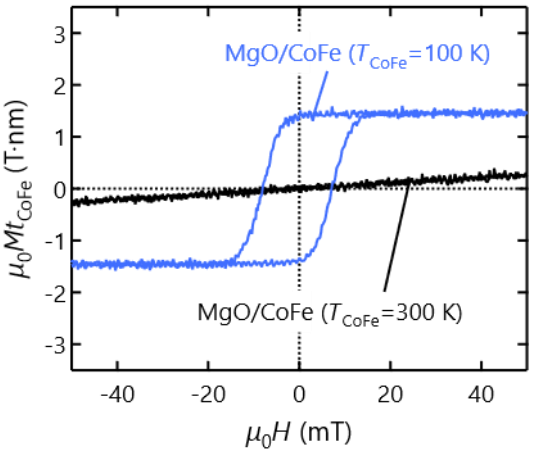

Fig. 1. Magnetization curves of a CoFe layer deposited on MgO at 300 or 100 K.

This study was partly based on the results obtained from a project, JPNP16007, subsidized by the New Energy and Industrial Technology Development Organization (NEDO).

References [1] T. Nozaki *et al.*, APL Mater. **8**, 011108 (2020).

Microscopic study of MTJ degradation toward High-density STT-MRAM: Impact of interface Oxygen Frenkel defects in MgO barrier

Kioxia Corporation[1], Mie University[2], ◦Rina Takashima[1], Takeo Koike[1], Shogo Itai[1], Hideyuki Sugiyama[1], Young Min Lee[1], Masaru Toko[1], Soichiro Ono[1], Daisuke Watanabe[1], Soichi Oikawa[1], Katsuhiko Koi[1], Hiroyuki Kanaya[1], Kohji Nakamura[2], and Masahiko Nakayama[1]

E-mail: rina1.takashima@kioxia.com

Spin transfer torque MRAM (STT-MRAM) has attracted attention as a non-volatile memory device thanks to its high speed, high endurance, and low power consumption. Recent studies [1-3] have shown that STT-MRAM provides a way to realize a high-density memory by using magnetic tunnel junctions (MTJs) with small diameter. One of the crucial technologies for achieving a scaled MTJ is to ensure the reliability of the barrier layer in a MTJ. Shrinking the MTJ diameter requires the reduction of resistance area product (RA) of a MTJ in order to supply enough current for write operations. RA reduction involves thinning the MgO barrier layer, which can cause resistance drift and degradation in tunnel magnetoresistance (TMR) ratio under an operating voltage [4]. Resistance drift and TMR degradation are critical issues as they lead to readout errors. The microscopic origin and effective methods to suppress the observed degradation have not been proposed.

In this study, we experimentally observed the stress-time-dependent resistance drift and TMR ratio degradation in MTJs with a diameter of 25 nm. The mechanism and suppression methods of the resistance drift and TMR ratio degradation were investigated using density functional theory (DFT), nonequilibrium Green function (NEGF) calculations, and a time-evolution model [5]. With microscopic calculations, we found that the degradation can be explained by current-induced generation of oxygen Frenkel defects at the interface of MgO and Fe (Fig. 1(a)). The impact of the initially formed oxygen vacancies in MgO was also investigated. It was found that the initial oxygen vacancies at the interface of MgO lower the formation energy of interface O Frenkel defect. Therefore, the reduction in the initial oxygen vacancies suppresses the resistance drift and TMR degradation by mitigating the generation of Frenkel defects (Fig. 1(b)). Our findings provide insights into improving reliability in high-density STT-MRAM.

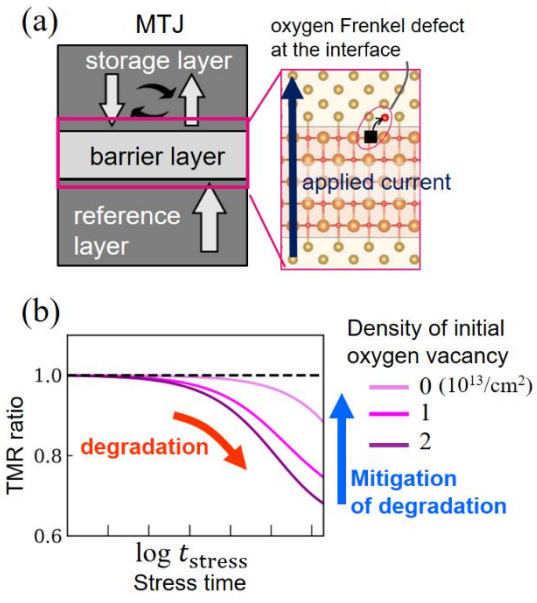

Figure 1 (a) Schematic of the oxygen Frenkel defects at the interface of the barrier layer, which cause the degradation. (b) Simulation results for stress-time dependence of TMR ratio [5]. (©2024 IEEE).

[1] S. M. Seo et al., 2022 IEDM, p. 218. [2] M. Nakayama et al., 2023 IEDM, 31-1. [3] H. Aikawa et al., 2024 IEDM, 20-1. [4] K. Hosotani et al., 2008 IRPS, p.703. [5] R. Takashima et al., 2024 IRPS, P10.EM.

Tunneling magnetoresistance and spin-orbit torque magnetization switching in ferrimagnetic Gd-Fe-Co based magnetic tunnel junction

東大院理[1],産総研新原理[2],東大物性研[3],東大 TSQS[4], ジョンズホプスキンス大[5]
柚木崎 正彦[1], 日比野 有岐[2], 井土 宏[1,3], Hanshen Tsai[1], 石橋 未央[1], 三輪 真嗣[3,4],
林 将光[1,4], 中辻 知[1,3,4,5]
Dep. Phys., Univ. Tokyo[1], AIST[2], ISSP, Univ. Tokyo[3], TSQS, Univ. Tokyo[4], JHU[5]
M. Yunokizaki[1], Y. Hibino[2], H. Idzuchi[1,3], H. Tsai[1], M. Ishibashi[1], S. Miwa[3,4],
M. Hayashi[1,4], S. Nakatsuji[1,3,4,5]

While magnetoresistive random-access memory using magnetic tunnel junctions (MTJs) has been commercialized, current research and development are focused on making the device faster by replacing the ferromagnetic layers with antiferromagnets, and ferrimagnets. Recent reports of 180 degree switching of magnetic moments in antiferromagnets [1] are promising for the development of MTJs. On the other hand, ferrimagnetic materials also show fast spin dynamics, especially near the magnetization compensation point, beneficial for high-speed operation of devices. However, there are a limited number of reports on MTJ using ferrimagnets. In this study, spin-orbit torque magnetization switching is studied in three-terminal magnetic tunnel junctions with a ferrimagnetic Gd-Fe-Co free layer [2].

Pt is used as a spin current generation layer and a Co-Fe-B synthetic antiferromagnet is used as the reference layer. A thin Fe-B layer is inserted between the Gd-Fe-Co free layer and the MgO barrier. The thickness of the Fe-B layer is varied from 0.4 to 1.2 nm. We find the tunnel magnetoresistance ratio increases with increasing Fe-B layer thickness until it saturates at ~14% (Fig. 1a). Current induced magnetization switching is studied using Kerr microscropy (Fig. 1b, 1c). We find the current density needed to reverse the magnetization of the Gd-Fe-Co/Fe-B layer via spin-orbit torque (Fig. 1b and 1c) changes little with the Fe-B layer thickness. The results highlight the effectiveness of the thin Fe-B layer in obtaining sizable tunneling magnetoresistance and efficient spin-orbit-torque switching.

This work was supported by JST-Mirai Program (JPMJMI20A1), and JST-ASPIRE (JPMJAP2317).

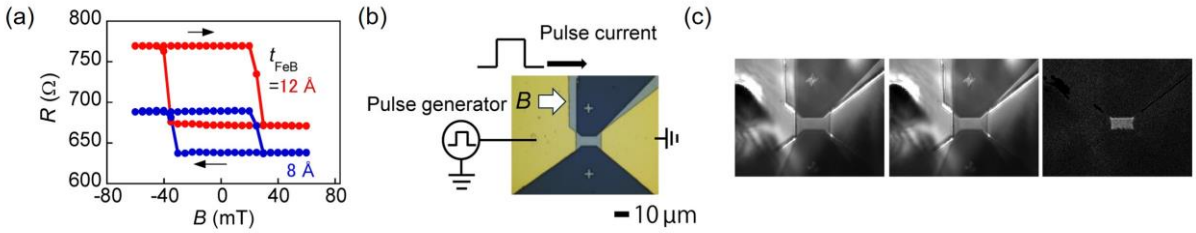

Fig. 1 (a) TMR curves for MTJ. (b) Photograph of the device and the measurement circuit diagram of SOT switching. (c) Kerr images before (left) and after (middle) a pulse is applied. The right image shows the differential image of the middle and left images, which confirms the switching of the ferrimagnet.

[1] T. Higo *et al*. *Nature* **607,** 474 (2022). [2] M. Yunokizaki *et al., Jpn. J. Appl. Phys.* **64,** 010904 (2025).

Size-Dependent Dynamic Properties of Stochastic Magnetic Tunnel Junction with a Synthetic Antiferromagnetic Free Layer

[O](M1) Takuma Kinoshita,[1,2] Ju-Young Yoon,[1] Nuno Caçoilo,[1] Haruna Kaneko, [1,2] Shun Kanai,[1-7] Hideo Ohno,[1,3,4,8] and Shunsuke Fukami[1-4,8,9]

[1] Lab. for Nanoelectronics and Spintronics, RIEC, Tohoku Univ.,
[2] Graduate School of Engineering, Tohoku Univ., [3] WPI-AIMR, Tohoku Univ.,
[4] CSIS, Tohoku Univ., [5] PRESTO, Japan Science and Technology Agency (JST),
[6] DEFS, Tohoku Univ., [7] National Institutes for QST,
[8] CIES, Tohoku Univ., [9] Inamori Research Institute for Science
E-mail: kinoshita.takuma.p2@dc.tohoku.ac.jp

Probabilistic computers (p-computers) consisting of stochastic magnetic tunnel junctions (s-MTJs) have emerged as a candidate for energy-efficient computers suitable for complex tasks[1][2]. For fast and reliable computation, s-MTJs require a high robustness against external fields and a short relaxation time τ. In this study, we investigate the size dependence of the external field robustness and τ in circular s-MTJs with a synthetic antiferromagnetic (SAF) free-layer. The stack of s-MTJ consists of, from the substrate side, Ta (5)/PtMn (20)/Co (2.00)/Ru (0.85)/CoFeB (2.20)/MgO (1.10)/CoFeB (1.80)/Ru (0.74)/CoFeB (2.34)/cap (nominal thicknesses in nm). The SAF-free layer consists of two CoFeB layers separated by the Ru layer, with their magnetizations compensating each other [3]. Figure 1(a) shows an example of a measured random telegraph noise signal with definitions of event times for antiparallel (AP) and parallel (P) states. Figure 1(b) shows the τ of the s-MTJs as a function of the electrically active diameter D_{ele}. The field robustness was evaluated using a slope of the τ_{AP} / τ_P vs $\mu_0 H$ curve (Fig. 1(c)) [3], and Fig. 1(d) shows its dependence on D_{ele}. We find that smaller s-MTJs exhibit shorter relaxation times and stronger field robustness, which are attributed to the reduced energy barrier between the AP and P states and the decreased Zeeman energy, respectively. This work provides guidelines for designing s-MTJs towards high-performance p-computers.

This work is partly supported by JSPS-KAKENHI, JST-CREST, JST-PRESTO, JST-ASPIRE, and MEXT X-NICS.

References

[1] K. Y. Camsari *et al.*, Phys. Rev. X **7**, 031014 (2017). [2] W. A. Borders *et al.*, Nature **573**, 390 (2019).
[3] K. Kobayashi *et al.*, Phys. Rev. Appl. **18**, 054085 (2022).

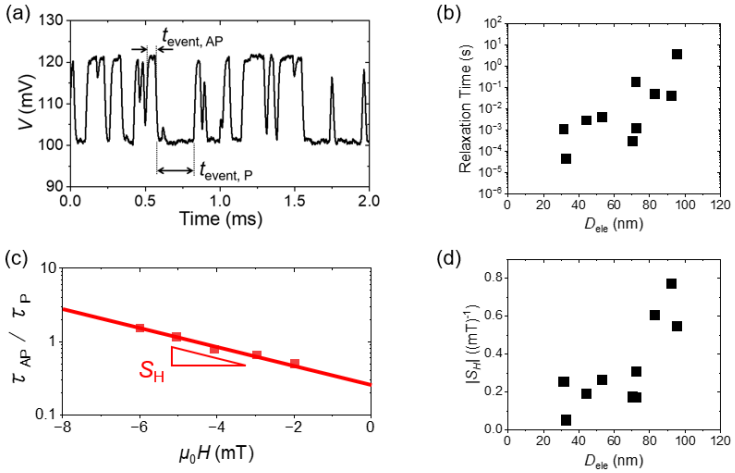

Fig.1 (a) An example of random teregraph noise and definitions of event times. (b) τ of the s-MTJs as a function of the D_{ele}. (c) An example of the τ_{AP} / τ_P as a function of the external field with the definition of S_H. (d) S_H as a function of the D_{ele}.

Determination of coupling states of a spin-torque oscillator in an HDD head using injection locking

東芝[1], NIMS[2] ○中川 裕治[1], 首藤 浩文[2], 桜庭 裕弥[2], 前田 知幸[1]

Toshiba[1], NIMS[2], ○Yuji Nakagawa[1], Hirofumi Suto[2], Yuya Sakuraba[2], Tomoyuki Maeda[1]

E-mail: yuji4.nakagawa@toshiba.co.jp

Spin-torque oscillators (STOs) with multiple oscillation layers improve their oscillation properties and functionalities by forming coupled states between the oscillation layers. In microwave-assisted magnetic recording (MAMR) [1], a key technology for increasing the recording capacity of hard disk drives (HDDs), an anti-parallel coupling of oscillation layers enables emission of a focused microwave magnetic field desirable for recoding [2]. We have developed an STO structure with two oscillation layers to obtain such a coupled oscillation state and reported spectrum measurement results from the STO fabricated in HDD recording heads that imply the coupled oscillation [3, 4]. However, conclusive experimental evidence of the coupling has not been obtained.

In this study, we developed an analysis method of the coupling state in an STO using injection locking and applied the method to an STO in a MAMR head. During the injection of an external microwave magnetic field (Fig. 1a), the STO resistance was monitored to detect injection locking [5]. By comparing the results of spectrum and injection locking measurements, we found that the coupled state did not respond to the injected microwave field (Fig. 1b). This is because the synchronization with the injected microwave field provides little benefit in the static energy due to the cancellation by the anti-parallel configuration of the two oscillation layers. This insensitivity to the microwave field also indicates that the coupled oscillation can mitigate the interaction problem between the STO and the HDD head structures, contributing to the stable oscillation and the generation of the focused microwave field only in the vicinity of the STO. On the other hand, the uncoupled state, where only one magnetic layer oscillates under the opposite current bias polarity, showed a clear injection locking because the synchronization between the oscillation and microwave field is energetically favorable. The frequency of the injection locking coincides with the oscillation peak observed in the spectrum measurement (Fig. 1c). These results provide evidence of the coupled oscillation in the STO for MAMR and demonstrate the capability of our method to determine the coupling state.

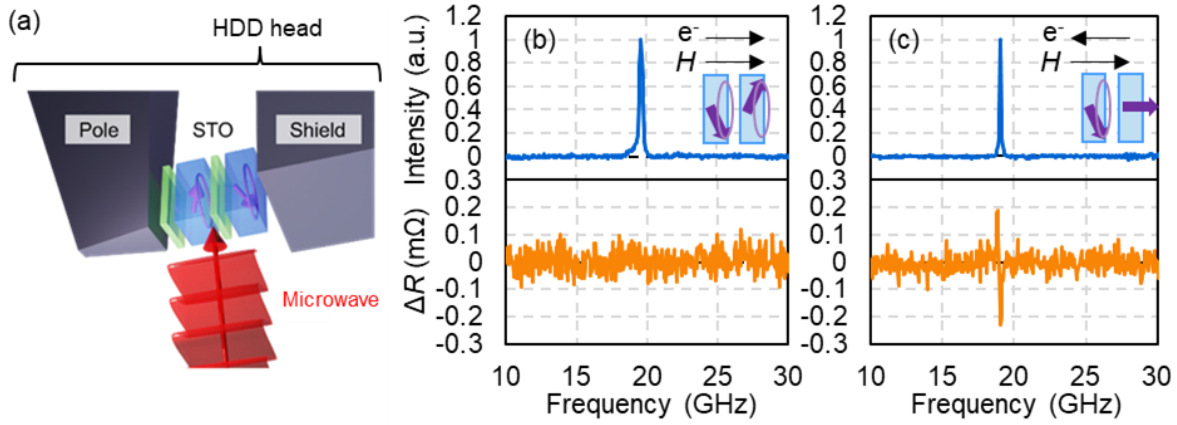

Fig.1 (a) Schematic illustration of the injection locking experiment. **(b, c)** Results of spectrum (top) and injection locking (bottom) experiments at coupled and uncoupled states, respectively.

References: [1] J.-G. Zhu *et al.*, *IEEE Trans. Magn.* **44**, 125 (2008). [2] M. Takagishi *et al.*, *IEEE Trans. Magn.* **57**, 3300106 (2021). [3] Y. Nakagawa *et al.*, *IEEE Trans. Magn.* **58**, 3201005 (2022). [4] Y. Nakagawa *et al.*, *Appl. Phys. Lett.* **122**, 042403 (2023). [5] N. Asam *et al.*, *Appl. Phys. Lett.* **119**, 142405 (2021).

High-sensitivity and hysteresis-free tunnel magneto-resistance sensor with magnetic vortex structure

[1]Graduate School of Engineering, Tohoku Univ., [2]CSIS, Tohoku Univ.
°Seiya Takano[1], Takafumi Nakano[2], Mikihiko Oogane[1,2]
* E-mail: seiya.takano.t5@dc.tohoku.ac.jp

Tunnel magnetoresistance (TMR) sensors utilizing magnetic tunnel junctions (MTJs) are high- sensitivity magnetic sensors capable of operating at room temperature [1]. In high-sensitivity magnetic sensors like TMR sensors, minimizing hysteresis error is critical to avoid measurement inaccuracies. However, when the free layer film has a multidomain structure, completely eliminating magnetic hysteresis is difficult. In order to resolve this problem, this study aims to develop hysteresis-free and high-sensitivity MTJ by employing magnetic vortex structure with hysteresis-free and microfabricated pillar-shaped pinned layer on that [2].

We deposited a multilayered MTJ film on a thermally oxidized Si substrate, consisting of Ta (5)/Ru (40)/Ta (5)/CoFeSiB (60)/Ta (0.2)/CoFeB (3)/MgO/CoFeB (3)/TaB (0.1)/CoFe (0.8)/Ru (0.8)/CoFe (3)/IrMn (10)/Ta (2)/Ru (7) (nominal thickness in nm) by magnetron sputtering. Then we microfabricated the film $2R_b$ = 10μm and $2r_t$ = 2μm where R_b is the free layer radius and r_t is the pinned layer radius. Subsequently, we conducted magnetic annealing process with 1T in plane magnetic field. TMR properties of the microfabricated films were measured by dc two-probe method.

We observed a liner and hysteresis-free magnetic conductance curves for the minor loop. The saturation field was reduced from 100 Oe to 16 Oe through the microfabrication of the pinned layer. The TMR ratio was 140%, resulting in a sensitivity of ca. 8%. These results suggest that the vortex-type TMR sensor with a microfabricated pinned layer is a promising approach for achieving a high-sensitivity and hysteresis-free TMR sensor. Since the pinned layer can be further miniaturized up to the 100 nm order, vortex-type TMR sensors are expected to exhibit higher sensitivity, with the potential to achieve a sensitivity improvement of ca. 100%/Oe.

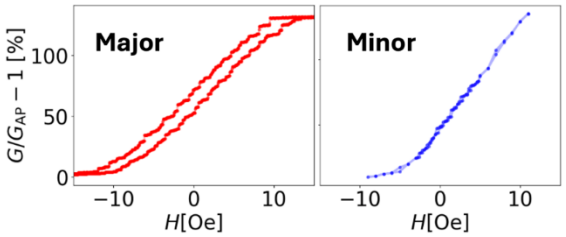

Fig. 1. The experimental conductance curves in the major and minor loops where $2r_t$ = 2μm.

This research was supported by the SIP Project, BRIDGE Project, SCOPE Project, X-nics Project, GP-Spin, CSIS, and CIES from Tohoku University.

References

[1] M. Oogane *et al.,* Appl. Phys. Express **14**, 123002 (2021).
[2] M. Endo *et al.,* J. Phys. D: Appl. Phys. **55**, 195001 (2022).